Cerebral Cortex April 2012;22:765–775
doi:10.1093/cercor/bhr110
Advance Access publication June 21, 2011

Cortical Network for Gaze Control in Humans Revealed Using Multimodal MRI

Elaine J. Anderson[1,2], Derek K. Jones[3,4], Ruth L. O'Gorman[5,6], Alexander Leemans[7], Marco Catani[5] and Masud Husain[1]

[1]UCL Institute of Cognitive Neuroscience, London WC1N 3AR, UK, [2]UCL Institute of Ophthalmology, London EC1V 9EL, UK, [3]Cardiff University Brain Research Imaging Centre, School of Psychology, Cardiff University, Cardiff CF10 3AT, UK, [4]Neuroscience and Mental Health Research Institute, Cardiff University, Cardiff CF10 3AT, UK, [5]Institute of Psychiatry, King's College London, London SE5 8AF, UK, [6]MR Center, University Children's Hospital, Zurich 8032, Switzerland and [7]Image Sciences Institute, University Medical Center Utrecht, Utrecht 3584 CX, the Netherlands

Address correspondence to Dr Elaine Joanna Anderson, UCL Institute of Cognitive Neuroscience, 17 Queen Square, London WC1N 3AR, UK. Email: e.anderson@fil.ion.ucl.ac.uk.

Functional magnetic resonance imaging (fMRI) techniques allow definition of cortical nodes that are presumed to be components of large-scale distributed brain networks involved in cognitive processes. However, very few investigations examine whether such functionally defined areas are in fact structurally connected. Here, we used combined fMRI and diffusion MRI–based tractography to define the cortical network involved in saccadic eye movement control in humans. The results of this multimodal imaging approach demonstrate white matter pathways connecting the frontal eye fields and supplementary eye fields, consistent with the known connectivity of these regions in macaque monkeys. Importantly, however, these connections appeared to be more prominent in the right hemisphere of humans. In addition, there was evidence of a dorsal frontoparietal pathway connecting the frontal eye field and the inferior parietal lobe, also right hemisphere dominant, consistent with specialization of the right hemisphere for directed attention in humans. These findings demonstrate the utility and potential of using multimodal imaging techniques to define large-scale distributed brain networks, including those that demonstrate known hemispheric asymmetries in humans.

Keywords: fMRI, saccades, tractography

Introduction

It is now widely accepted that many cognitive functions are underpinned by large-scale brain networks connecting distributed cortical regions, some of which are highly lateralized to the left or right hemisphere in humans (Mesulam 1981; Goldman-Rakic 1988; Catani and ffytche 2005). Establishing how the cortical nodes within such networks are interconnected is likely to be crucial for understanding their functional significance. However, until the recent development of advanced imaging methods, we have gained little direct knowledge on network connectivity within the human brain.

Instead, we have largely relied on information from anatomical tracer studies in nonhuman primates to infer patterns of connectivity in the human brain. Indeed, white matter tracts that have been described in detail in macaque monkeys (Schmahmann and Pandya 2006) are often cited as if they are known to exist in humans, but for the main, have yet to be confirmed. Until recently, the only way to identify white matter anatomy in humans was through postmortem dissection and histological analysis of white matter fibers. However, with recent advances in diffusion magnetic resonance imaging (MRI) tractography, it is now possible to perform "virtual dissections" of the living human brain to visualize large-scale connectivity maps (Mori et al. 1999; Basser et al. 2000; Catani et al. 2002; Sporns et al. 2005; Hagmann et al. 2008; Jones 2008). Yet, very few investigations have examined how cortical regions defined on the basis of their functional activation are structurally connected.

Here, we combined tractography with functional MRI (fMRI) to investigate structural connections between nodes in the cortical network for gaze control in humans. This system is of fundamental importance as oculomotor responses can be used to probe many aspects of cognitive control (Kennard et al. 2005; Sweeney et al. 2007) including spatial working memory (Husain et al. 2001; Brignani et al. 2010), visual search and attention (Binello et al. 1995; Mannan et al. 2005) as well as top-down control related to response initiation and suppression (Sumner et al. 2006; Anderson et al. 2008). It is now well established in nonhuman primates that a distributed network, including the frontal eye field (FEF) in the dorsolateral frontal cortex (Bruce et al. 1985; Huerta et al. 1987), supplementary eye field (SEF) located in dorsomedial frontal cortex (Russo and Bruce 2000), and parietal eye field (PEF) within the lateral intraparietal (LIP) area (Thier and Andersen 1998; Goldberg et al. 2002), is crucial for saccadic eye movement control (for a review, see Johnston and Everling 2008). Moreover, anatomical tracer studies have demonstrated that these areas are heavily interconnected, both within and across hemispheres (Stanton et al. 1993, 1995; Schall et al. 1995).

The human homologues of these regions have been extensively documented using high-resolution neuroimaging techniques (Paus 1996; Grosbras et al. 1999; Tehovnik et al. 2000; Lobel et al. 2001; McDowell et al. 2008; Amiez and Petrides 2009), but despite substantial literature on their location and function, the underlying pattern of connections remains to be established. Investigations of oculomotor control in clinical populations have also highlighted a number of deficits that might, in part, be ascribed to pathological changes in white matter pathways (Broerse et al. 2001; Gooding and Basso 2008) and observations in patients with brain lesions have suggested right hemisphere specialization for directed attention, a process that is intimately linked to gaze control (Posner et al. 1984; Rafal 1994; Mesulam 1999). Hence, mapping the structural connections that exist within the healthy human brain will help our understanding of the changes in circuitry that might explain such deficits.

Typically, previous attempts to infer structure–function relationships in the human brain have used tractography to identify pathways connecting anatomically defined regions, followed by post hoc interpretation of their functional significance based on previously published functional data.

Alternatively, fMRI has been used to identify cortical areas associated with a specific cognitive function and then assumptions about the underlying structural connections have been made. However, by combining tractography and fMRI within the same group of subjects, it should be possible to identify "maps of connections" implicated in a specific cognitive function (Rykhlevskaia et al. 2008).

To date, there are very few multimodal imaging studies that have combined these 2 techniques within the same subjects (e.g., Kim and Kim 2005; Saur et al. 2008; Staempfli et al. 2008; Lanyon et al. 2009), and these investigations have typically used the single approach of constraining fiber reconstruction algorithms to dissect pathways connecting functionally defined regions. Here, to advance on these methods, we combined tractography and fMRI in 10 healthy volunteers, using a 2-stage analysis. For each individual, we initially ran an anatomically guided tract reconstruction (independent of the fMRI data), which ensured no loss of information by taking into account the variability that exists in individual anatomy. This was followed by a second stage in which individual fMRI data were used to constrain the tractography results. In addition, we created a group-averaged diffusion MRI data set to obtain a group-averaged tractography result to further explore the anatomy that might generalize to the population.

Materials and Methods

Participants

Ten participants (4 males), all right handed (mean age 29 ± 3 years), with normal visual acuity, and no history of neurological or psychological disorder, gave informed written consent to take part in this study. This study was approved by Hammersmith Ethics Committee.

Each participant underwent 4 consecutive scans in a single session, using a GE 1.5-T Signa NV/i LX MRI system (General Electric, Milwaukee, WI), with standard quadrature birdcage head coil: 1) diffusion-weighted echo planar imaging (EPI), 2) functional EPI—eye-field localizer A, 3) functional EPI—eye-field localizer B, and 4) T_1-weighted structural scan.

Diffusion Tensor–MRI Acquisition

A multislice diffusion-weighted EPI sequence, fully optimized for diffusion tensor imaging of white matter (Jones, Williams, et al. 2002), was carried out on all subjects. Full brain coverage was achieved with 60 near-axial slices, with isotropic resolution (voxel size 2.5 × 2.5 × 2.5 mm, field of view 240 × 240 mm, acquisition matrix 96 × 96, interleaved slice order). The duration of the diffusion-encoding gradients was 17.3 ms, giving a maximum diffusion weighting of 1300 s mm^{-2}. Diffusion gradients were applied in 64 isotropically distributed orientations. The acquisition was gated to the cardiac cycle using a peripheral gating device placed on the subjects forefinger. Depending on the individual heart rate, an effective TR was selected that allowed at least 180 ms per image, that is, enough time to collect, reconstruct, and save each slice. Scan time was ~20 min, depending on heart rate.

Analysis of Diffusion Tensor–MRI data

After correction for the image distortions introduced by the application of the diffusion-encoding gradients (Leemans and Jones 2009), the diffusion tensor was determined in each voxel following the method of Basser et al. (1994). From the diffusion tensor data, information about the average diffusivity, diffusion anisotropy, and the principle direction of diffusion can be calculated (Basser and Pierpaoli 1996; Basser et al. 2000). The Diffusion Tensor–MRI (DT-MRI) data were coregistered to each individual's structural scan and registered in Montreal Neurological Institute (MNI) stereotactic space for consistency with the fMRI data. The fractional anisotropy (FA) was computed in each voxel, highlighting the boundary between white and gray matter. This "FA map" was used to define the regions of interest (ROIs) used in the tractography process.

To ensure that no hemispheric bias could have been imposed by the observer whilst defining the ROIs, half of the diffusion MRI data sets were flipped along the midline (as well as their corresponding anatomical and fMRI data) before the ROIs were defined. Information about which data sets were flipped was not revealed to the observer until after the analysis was complete, at which point all data sets were returned to their original orientation for statistical analysis and presentation of the results.

Group Averaged DT-MRI Data Set

A group-averaged DT-MRI data set was generated from all 10 participants. The (unflipped) tensor data for each participant was spatially normalized and coregistered to the standard T_2-weighted MNI EPI template, included as part of SPM99 (Wellcome Trust Centre for Neuroimaging, UCL, www.fil.ion.ucl.ac.uk), using the approach described by Alexander et al. 1999, which employs the Automated Image Registration (AIR) package for coregistration (Woods, Grafton, Holmes, et al. 1998; Woods, Grafton, Watson, et al. 1998). Full details of the spatial normalization and coregistration procedure and generation of the average DT-MRI volume are described in Jones, Griffin, et al. (2002).

Eye-Field Localizer and fMRI Acquisition

All subjects underwent 2 functional EPI scans to localize the cortical eye fields. Subjects were required to perform blocks of large self-paced horizontal saccades in the dark for 30 s, followed by 30 s of rest, in which they maintained a steady central eye position. A practice session prior to scanning was completed by all subjects to ensure they could perform the task correctly. The location of the cortical eye fields differs according to task requirements, stimulus type, and the oculomotor response required (McDowell et al. 2008). For these reasons, we used an oculomotor paradigm that minimized target-related effects and hence minimized activity unrelated to generating and carrying out a saccade. Aural instructions were given via MRI compatible headphones instructing participants when to "start" and "stop" making eye movements.

T_2^*-weighted images were acquired using Gradient Echo EPI (128 × 128 matrix, FOV 240 × 240 mm, time echo [TE] 40 ms and 90° flip angle). Full brain coverage was achieved with 28 near-axial slices (4.5-mm slice thickness with a 0.5-mm gap, interleaved slice order, in-plane resolution 1.9 × 1.9 mm). Participants performed 2 identical scan runs, each lasting 8 min (96 volumes per scan, TR 5 s). Each scan started with a 30 s "rest" block (6 volumes), followed by a 30 s "eye movement" block (6 volumes), repeated 8 times.

A T_1-weighted anatomical scan with 1.5-mm slice thickness and 0.86 × 0.86 in-plane resolution (after zero filling) was also acquired for every participant using an axial 3D SPGR sequence (256 × 256 matrix, FOV 220 × 176, TR 159 ms, TE 5.2 ms, 20° flip angle).

Analysis of fMRI Data

All imaging data were analyzed using SPM2 (www.fil.ion.ucl.ac.uk). For the individual analyses, half of the fMRI data sets were flipped along the midline prior to preprocessing—corresponding to those participants who had their DT-MRI data sets flipped. The corresponding structural scan was also flipped. This was to ensure that no hemisphere bias was imposed by the observer when defining the ROIs.

For each subject, all images were realigned to the first image to compensate for head movement, coregistered to the participant's T_1 structural image, and spatially smoothed with a 7-mm isotropic Gaussian smoothing kernel. For the group analysis (no data sets were flipped), all images for each subject were realigned to the first image, spatially normalized to the SPM EPI template, and spatially smoothed with a 7-mm isotropic Gaussian smoothing kernel.

For each individual, linear regressors representing the time series for blocks of eye movements and blocks of rest were convolved with

a synthetic hemodynamic response function and its temporal derivative. The general linear model, as employed by SPM2, was used to generate parameter estimates of activity for each regressor at every voxel. A linear contrast between regressors identified those voxels with greater activity during blocks of eye movements compared with rest, thus revealing the locus of the cortical eye fields in each subject. A threshold of $P < 0.001$ uncorrected was used to determine significance.

For the group data, a random effects analysis was performed (Friston et al. 1999). A single mean image representing "eye movements versus rest" for each subject was used as the basis for interparticipant comparisons and used to generate a statistical parametric map of the *t* statistic at every voxel (Fig. 1). A threshold of $P < 0.001$ uncorrected was used to determine significance.

Anatomically Defined ROIs

For stage 1 of the analysis, all ROIs were defined on axial slices of the FA map, which clearly highlights the boundary between white and gray matter (Fig. 2). Initially, for all subjects, 2 large ROIs were defined in the superior frontal lobe (SEF ROI) and middle frontal lobe (FEF ROI) of each hemisphere, using anatomical landmarks for guidance. ROIs were defined to encompass a large region of white matter lying directly beneath regions of cortex known to include the human SEF and FEF. For the FEF ROI, a region of white matter underlying the middle and superior frontal gyrus, lateral to the internal capsule, and anterior to the central sulcus, was defined (approximate Brodmann areas [BAs] 44, 8, 6, and 4). The approximate MNI coordinates for this region ranged in the *X* direction from 25 to 60, in the *Y* direction from –10 to 25, and from 20 to 60 in the *Z* direction. These coordinates varied depending on individual anatomy. For the SEF region, a region of superior frontal cortex medial to the internal capsule and anterior to the central sulcus, underlying the precentral gyrus (BAs 4 and 6), was defined (approximate *X* range: 4–20, *Y* range: –15 to 10, *Z* range: 45–70).

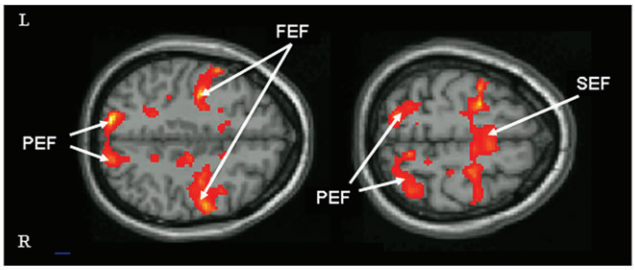

	Region		x/y/z	Z	BA
Frontal	FEF	R	52/-6/46	4.22	4
			40/-8/50	4.14	6
			26/-8/52	4.11	6
		L	-60/4/38	4.41	6
			-38/-10/44	4.39	6
			-26/-8/52	4.31	6
	SEF	R	2/-6/70	4.52	6
		L	-2/-6/70	4.02	6
Parietal	PEF	R	10/-56/58	4.34	7
			24/-62/58	3.17	7
			36/-56/62	3.45	7
		L	-18/-66/62	3.74	7
			-26/-56/58	3.16	7

Figure 1. Functionally defined cortical eye fields. The cortical eye fields were localized in each participant using a standard saccadic eye movement paradigm (see Materials and Methods). Group normalized data are presented here, illustrating regions of the brain where activity was greater during blocks of saccadic eye movements in the dark compared with a central fixation baseline. Random effects analysis at $P = 0.001$ was used to determine coordinates of activation maxima, *Z* scores and approximate BAs as given above. A threshold of $P = 0.005$ has been used for illustration purposes only.

A further ROI was then defined within the parietal lobe of each hemisphere, encompassing a large area of white matter underlying all regions of the intraparietal sulcus (IPS) known to be involved in saccadic eye movements—that includes IPS 1, 2, and 3 (Sereno et al. 2001; Schluppeck et al. 2005, 2006; Levy et al. 2007; Anderson et al. 2008). More specifically, the PEF ROI started at the level of the corpus callosum inferiorly and included all white matter posterior to the occipitotemporal border (where regions BA 19 and 39 meet, MNI $Y \approx -60$), extending from the cuneaus on the medial side to the angular gyrus laterally and from the middle occipital gyrus inferiorly to the inferior aspect of the IPS as well as extending anteriorly along the IPS (approximate *X* range: 0–45, *Y* range: –50 to –90, *Z* range: 30–60).

For the group analysis, similar anatomical ROIs were defined on the group-averaged FA map and used as seed points for running tractography on the group-averaged DT-MRI volume.

Functionally Redefined ROIs

For stage 2 of our analysis, we redefined our regions using each individual's fMRI data. Using visual markers, the original large anatomically defined ROIs were refined to only include regions of white matter that lay directly beneath areas of cortical activity. These ROIs were smaller in size and more closely respected the anatomical locality of the individual's eye fields. The same tractography algorithms were then rerun for these new ROIs and the reconstructed streamtube data visualized in 3D along with the fMRI data. From this interactive 3D visualization, we were able to confirm whether the dissected pathways accurately reached areas of cortical activity.

Similar to the individual analyses, the large anatomically defined ROIs used for the group analysis were refined using the group normalized fMRI results and tractography rerun on the group-averaged DT-MRI volume.

Tractography Algorithm

White matter fiber trajectories were reconstructed and visualized in 3D using in-house software based on the procedure originally described by Basser et al. (2000). Whole brain tractography was performed, by seeding tracts from every vertex of a 2 × 2 × 2 mm grid superimposed on the brain. For each of these seed points, the principal eigenvector was calculated from the DT data (i.e., the direction of greatest diffusivity), which was treated as being tangential to the trajectory of the tract. Each fiber trajectory was reconstructed by propagating a streamline bidirectionally from an initial seed point in the direction of the principal eigenvector for 0.5 mm and then recomputing the principal eigenvector at the next location. The algorithm then moved a further 0.5 mm along this new direction. The tracking process continued tracing a pathway in this manner until the FA of the tensor fell below a fixed arbitrary threshold (set to 0.2). This threshold consistently differentiated between white and gray matter when windowing the FA image.

Only those trajectories that passed through 2 predefined ROIs, defined on the FA images, were retained for analysis. Using this 2-ROI approach, tractography was used to reconstruct all fibers passing through any 2 of our spatially distinct ROIs. In particular, we were interested in dissecting tracts which connect 1) SEF and FEF, 2) FEF and PEF, and 3) SEF and PEF. The dissected tracts were visualized in 3D as "streamtubes," using the mathematical software package MATLAB (The Mathworks, Natick, MA) (Zhang et al. 2003). This 3D visualization could also be displayed simultaneously with the FA volumes, sliced into axial, coronal, and sagittal planes, with or without superimposed fMRI activity and viewed interactively from any angle to facilitate identifying the neuroanatomical location of the tract reconstructions.

For each dissected pathway, we computed the number of reconstructed streamlines (RS) and the mean FA.

Results

First, we obtained diffusion-weighted EPI brain scans on 10 healthy volunteers (all right handed), using a sequence fully

optimized for diffusion MRI tractography (Jones et al. 1999). In addition, we functionally identified the cortical eye fields in each of our 10 subjects using functional MRI and a standard eye movement paradigm (see Materials and Methods) (Fig. 2). One subject had very little cortical activity above threshold in any brain area and was therefore discarded from the individual analysis. For the remaining 9 subjects, we carried out a 2-stage process for dissecting the white matter tracts connecting the cortical eye fields.

Stage 1: Diffusion MRI–Based Tractography Reconstruction of the Connections between Anatomically Defined Frontal Oculomotor Regions

In this analysis, we reconstructed the white matter pathways of interest independently from the fMRI results. By using only anatomical landmarks, we were able to visualize frontal connections both within and across hemispheres. This analysis allowed us to explore the individual anatomy of the white matter pathways and therefore assess interindividual variability in patterns of connections. We first defined 2 large ROIs within the dorsolateral and dorsomedial prefrontal cortex of each hemisphere for all subjects. These regions were defined on the individual FA maps, using anatomical landmarks for guidance and were drawn to encompass white matter underlying regions of cortex known to include the FEF and the SEF. For full details of the location and extent of the ROIs defined, see Materials and Methods. Whole brain tractography was then performed (seeding tracts from every vertex of a 2 × 2 × 2 mm grid superimposed on the brain), but only those trajectories that passed through both ROIs were retained for analysis (Conturo et al. 1999; Catani et al. 2002). In this way, we dissected the white matter pathways between the FEF and SEF within each hemisphere, as well as the pathway between the right and left SEF across hemispheres.

Comparing the number of voxels within each ROI for the right and left hemisphere confirmed there was no significant difference in region size between hemispheres for the FEF (t_8= 0.527, P = 0.613) or SEF (t_8 = –0.265, P = 0.798). Using these ROIs, we were able to dissect white matter pathways directly connecting the dorsomedial ROI (SEF) and the dorsolateral ROI (FEF) within each hemisphere for all 9 subjects, as well as a pathway connecting the right and left SEF via the anterior body of the corpus callosum. The dissected pathways were viewed in 3D, simultaneously with each individual's fMRI data and superimposed on intersecting axial and coronal slices of the FA map—allowing the origin, course, and termination of each pathway to be determined (Fig. 3*A*). For all 9 subjects, the path between the SEF and FEF in both hemispheres accurately terminated in regions of cortical activity, as did the pathway connecting the right and left SEF across hemispheres. Interestingly, the number of RS in this pathway was significantly higher in the right hemisphere than the left (t(8) = 2.770, p = 0.024) (Fig. 4). Note—this is despite there being no hemispheric bias in the size of the ROIs (as reported above).

In addition to the reconstructed pathways that accurately terminated within regions of cortical activity, there were also a number of pathways that projected to adjacent areas. This is not unexpected given the large size of our initial ROIs. To ensure that the hemispheric bias remained reliable and robust

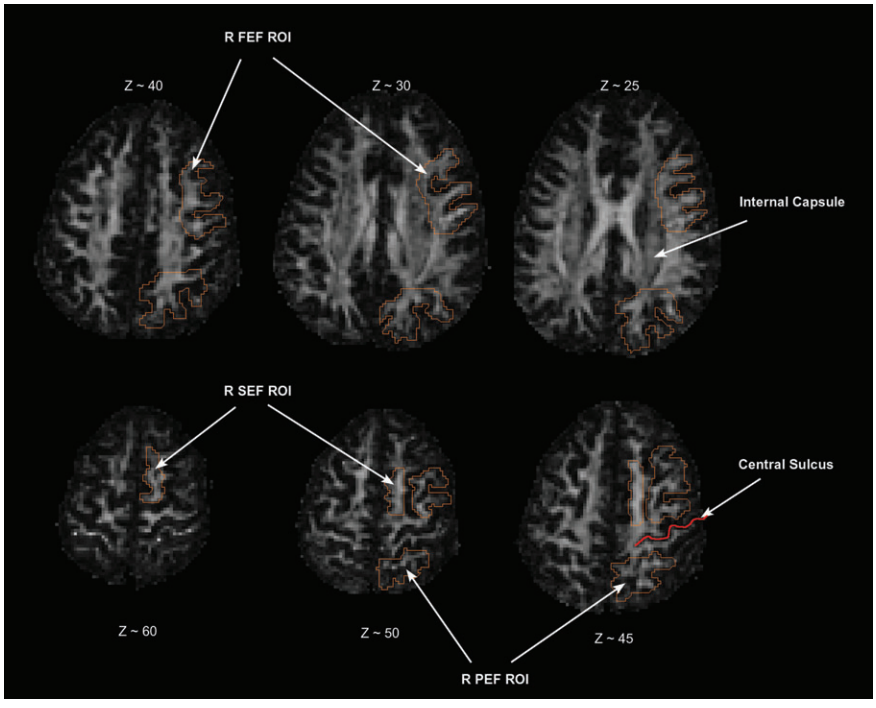

Figure 2. Anatomical definition of the ROIs. For stage 1 of the analysis, all ROIs were defined on the individual FA maps, using anatomical landmarks for guidance and were drawn to encompass white matter underlying regions of cortex known to include the FEF, SEF, and PEF. Selected axial slices of the FA map for a representative subject are illustrated above, with voxels to be included in the right FEF, SEF, and PEF ROIs outlined in orange. Note that the frontal and parietal ROIs do not cross the central sulcus (red line) and the FEF and SEF ROIs do not cross the internal capsule. For clarity, not all slices are illustrated in this figure—for full details of the *X*, *Y*, and *Z* ranges included in each ROI, see Materials and Methods. The *Z* coordinates given are approximate, as the individual FA maps were not normalized to the MNI template for the individual subject analyses.

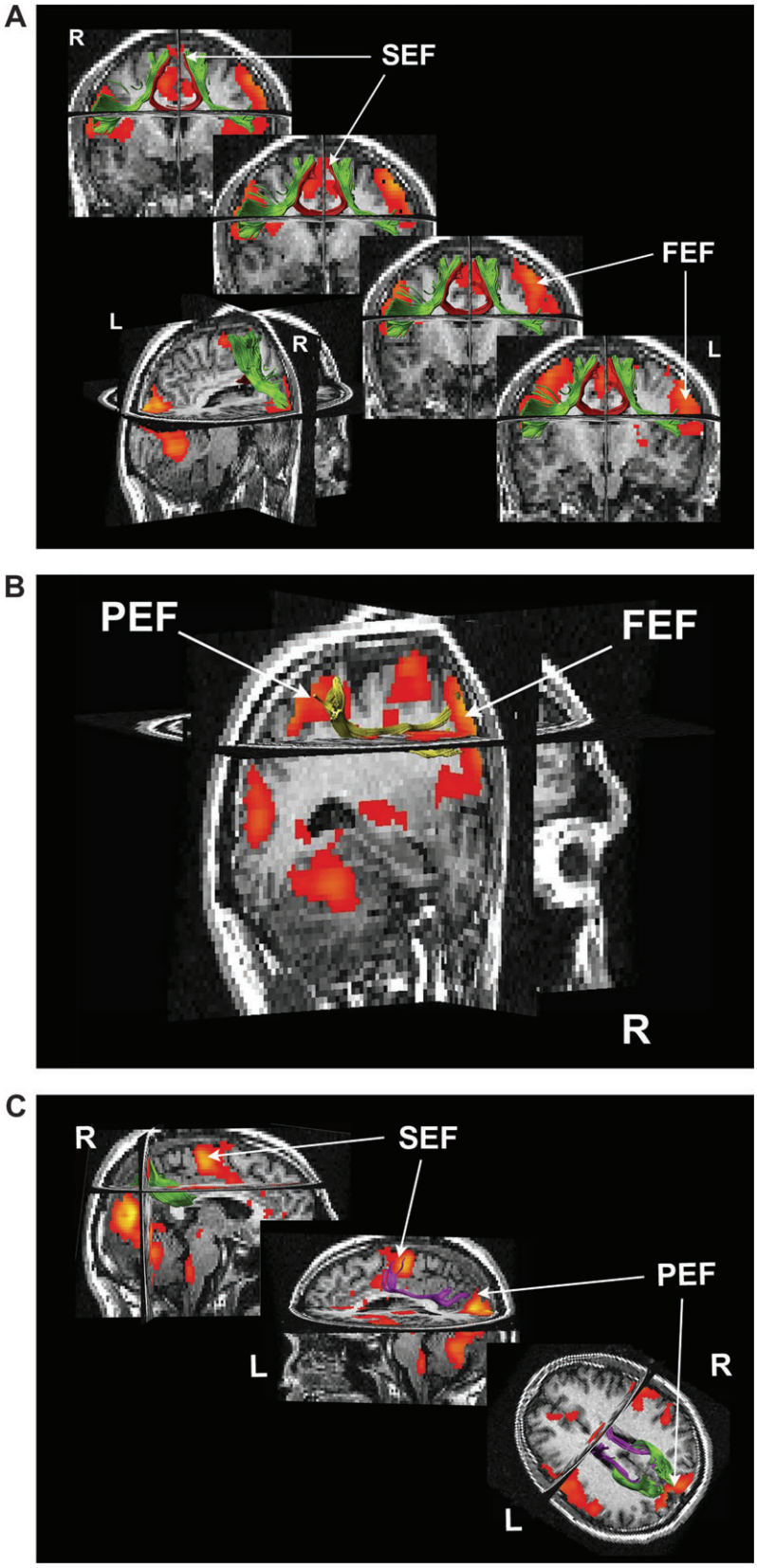

Figure 3. Combined DT tractography and fMRI for a single subject. For a representative subject, reconstructed tracts are illustrated in 3D superimposed on coronal, axial, and sagittal slices of the individual's anatomical image, together with their fMRI data (illustrated at $P = 0.005$). (*A*) Connections within the frontal lobes—contralateral SEF to SEF tract illustrated in red, ipsilateral SEF to FEF tracts in green. (*B*) Lateral frontoparietal pathway—dorsolateral tract connecting the right FEF and inferior parietal cortex in yellow. (*C*) Medial parietal connections—tract connecting ipsilateral SEF and PEF in magenta and contralateral PEF to PEF connection in green. This figure was generated using "ExploreDTI" (Leemans et al. 2009).

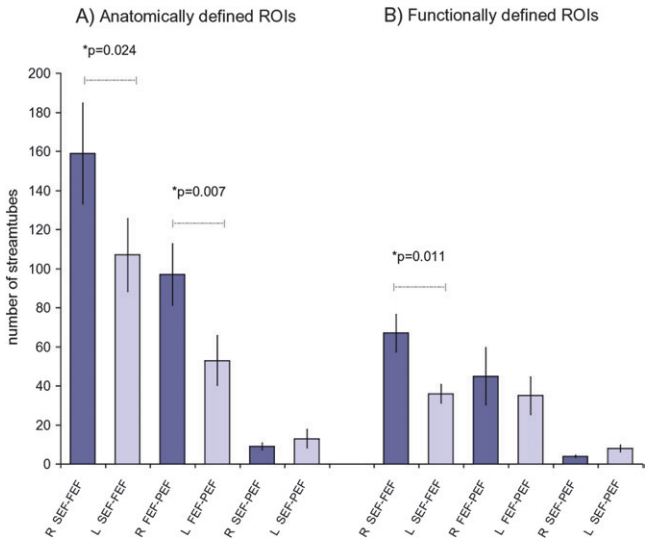

Figure 4. Histogram showing the number of reconstructed streamtubes in each tract. Group mean number of streamtubes in each reconstructed tract for (*A*) anatomically defined seed regions, (*B*) functionally redefined seed regions (see Materials and Methods). Error bars indicate standard error of the mean.

for only those pathways that accurately terminated within the functionally defined FEF and SEF, we performed a second stage of analysis in which our original ROIs were redefined using each individual's fMRI activity for guidance. We then reran the tractography using these new ROIs.

Stage 2: Tractography Constrained Using Frontal fMRI Activity to Redefine Seed Points

For the second stage of analysis, we refined the anatomical ROIs to only include voxels of white matter lying directly beneath the functionally defined FEF and SEF for each individual (a threshold of $P < 0.001$ uncorrected was applied to each individuals fMRI data to determine significance). There was no significant difference in ROI volume between the new right and left FEF ROI ($t_8 = 0.478$, $P = 0.647$) or SEF ROI ($t_8 = 0.049$, $P = 0.962$).

Using these new functionally defined ROIs, we reran our tractography analysis. The original reconstructed pathways were all found to be reliable, and although there were now fewer RS within each pathway, the right hemisphere lateralization remained significant for the SEF to FEF connection (Fig. 4*B*) ($t_8 = 3.407$, $P = 0.011$). Furthermore, for each subject, we obtained the mean value of the FA sampled along each pathway. This is a scalar measure that reflects the degree to which the diffusivity depends on the orientation in which it is measured and therefore considered an index reflecting microstructural organization (e.g., cohesiveness, ordering, etc.) and biological properties (e.g., degree of myelination, membrane permeability, etc.) of fibers (Beaulieu 2002). Although there were no significant differences between the 2 hemispheres at a threshold of $P = 0.05$, there was a trend for the mean FA to be larger on the right than the left for the SEF to FEF tract ($t_8 = 1.967$, $P = 0.085$).

Anatomical and fMRI-Constrained DT Tractography of the Frontoparietal Connections

Posterior projections from the FEF to the LIP area in the IPS have also been identified in nonhuman primates (Huerta et al. 1987; Blatt et al. 1990; Schall et al. 1995; Stanton et al. 1995). Hence, having successfully reconstructed white matter pathways connecting the 2 eye fields of the frontal cortex in our 9 subjects, we then sought to determine whether posterior projecting pathways could also be established.

The human homologue of monkey LIP is thought to lie within the IPS (Sereno et al. 2001; Schluppeck et al. 2005, 2006; Levy et al. 2007), where topographically organized areas associated with saccadic eye movements have been identified. Therefore, using the same methods as before, we initially defined a large parietal ROI in the white matter underlying the proposed location of the human PEFs in both hemispheres. Statistical analysis confirmed there was no significant difference in the size of the right and left parietal ROIs ($t_8 = -0.231$, $P = 0.823$). Using the same 2-ROI approach, we attempted to dissect white matter tracts connecting the FEF to PEF and the SEF to PEF within each hemisphere, as well as a tract connecting the right and left PEF across hemispheres.

We were able to reconstruct a dorsal frontoparietal tract connecting the FEF ROI to a posterior parietal region in both hemispheres, for all 9 subjects (Fig. 3*B*). This pathway consistently had a greater number of RS in the right hemisphere compared with the left ($t_8 = 3.566$, $P = 0.007$) (Fig. 4*A*). However, examining the reconstructed pathway in 3D along with the fMRI data revealed that this pathway did not project to a region of parietal cortex consistently activated by our oculomotor task (when a standard threshold for significance was applied: $P < 0.001$). Instead this pathway terminated in a more lateral region of cortex, known to be involved in visually guided oculomotor tasks (Perry and Zeki 2000; Mort, Perry, et al. 2003; Petit et al. 2009). The parietal ROIs used as seed points for the tractography were defined anatomically to include white matter underlying all regions of the IPS known to be involved in saccadic eye movements—that includes IPS 1, 2, and 3 (Sereno et al. 2001; Schluppeck et al. 2005, 2006; Levy et al. 2007; Anderson et al. 2008). Hence, this ROI extended from posterior to anterior ends of the IPS, thereby incorporating white matter associated with this dorsolateral frontoparietal tract (see Discussion).

A dorsomedial pathway connecting the SEF and PEF ROIs, via the cingulum, was also found for all subjects in the left hemisphere, but for only 6 subjects in the right hemisphere, although there was no consistent hemisphere bias in the number of streamtubes ($t_8 = 0.645$, $P = 0.540$) (Figs. 3*C* and 4*B*). Finally, as expected, there was a U-shaped tract connecting the contralateral PEF via the posterior body of the corpus callosum (Fig. 3*C*). All of these tracts accurately terminated in regions of cortical activity.

When the tractography was rerun using the more conservative ROIs defined by fMRI data, only ~50% of fibers within the large pathway connecting the FEF to lateral parietal cortex survived, and the rightward hemisphere bias was abolished ($t_8 = 0.635$, $P = 0.546$) (Fig. 4*B*). In contrast, the more variable pathway connecting the SEF and PEF did survive, but due to this pathway not being reconstructed in all subjects, we cannot make reliable statistical inferences. Furthermore, there was no significant hemisphere bias in the mean FA for either the FEF to PEF pathway ($t_8 = -1.208$, $P = 0.272$) or the SEF to PEF pathway ($t_8 = -1.207$, $P = 0.294$).

Group Average Analysis of the Diffusion and fMRI data

Lastly, we created a group average diffusion MRI data set to obtain a group-averaged tractography result (Jones, Griffin, et al. 2002). Group-averaged tractography has the advantage of providing a smooth and continuous trajectory representing the "central" location of the white matter pathways within the group, from which we can derive assumptions about the connections of the cortical eye fields within the general population. A further advantage of the group analysis is that the data are normalized and coregistered to a common space (MNI space, which approximates to the space of Talaraich and Tournoux), which allows for easy comparison with previously published coordinates for the location of the human cortical eye fields, as well as allowing our reconstructed pathways to be assigned to currently established white matter pathways.

We reran the tractography using the same 2-ROI approach as before, to obtain a group-averaged tractography result for connections between the SEF, FEF, and PEF. As before, the reconstructed tracts were visualized in 3D together with the group-averaged fMRI results (Fig. 5). Consistent with the individual data, within the frontal lobes there was a direct pathway connecting the ipsilateral FEF and SEF which was right hemisphere lateralized (number of streamtubes: right:left = 2.60:1). There was also a direct tract connecting the contralateral SEF via the corpus callosum (Fig. 5*A*). Posterior projections from the FEF were similar to those obtained for the large anatomically defined ROIs in the individual data sets, with a dorsal pathway connecting the FEF and a lateral area of parietal cortex. Similar to the individual data, this tract was also right hemisphere lateralized (number of streamtubes: right:left = 2.55:1), and once again did not appear to terminate in a region of cortex activated by our eye movement localizer (coordinates of tract end point: R and L [±39/−58/46], homologous BA 39/40) (Fig. 5*B*) but, is known to be involved in visually guided saccades. Hence, this right lateralized tract, which appears to generalize to the population, may also play a role in oculomotor control. For the group data, we were not able to reconstruct the medial tract connecting the SEF and PEF that had been evident in a subset of our individual data sets.

Discussion

By combining fMRI and diffusion MRI–based tractography, we have reconstructed the candidate white matter pathways linking functionally specified oculomotor areas in the human brain. Our data confirms some degree of homology with white matter connections known to exist in macaque monkeys but also highlights important characteristics unique to humans, particularly with respect to hemispheric differences.

For all individuals, we reconstructed pathways between the right and left SEF that passed through the anterior body of the corpus callosum (Figs 3*A* and 5*A*) and the right and left PEF via the posterior body of the corpus callosum (Figs 3*C* and 5*B*). There was also a direct pathway connecting the SEF to the ipsilateral FEF in both hemispheres, but importantly this was significantly lateralized to the right hemisphere (Figs 3*A* and 5*A*). In addition, we dissected a dorsal frontoparietal pathway, again more prominent in the right hemisphere, connecting the FEF to a region in the inferior parietal lobe (Figs 3*B* and 5*B*). Finally, we also found evidence for a frontoparietal pathway, projecting medially along the cingulum, connecting the SEF to the ipsilateral PEF, but this pathway was not demonstrable in all individuals (Fig. 3*C*).

Right hemisphere dominance in the gaze control network was found for all individuals (Fig. 4) and confirmed by the group average data set for both the SEF to FEF pathway, as well as the dorsal frontoparietal pathway connecting the FEF to the inferior parietal lobe. Such lateralization in the underlying anatomy might explain recent fMRI findings that demonstrate right hemisphere dominance in cortical activity in response to visually guided saccades (Petit et al. 2009). Consistent with these findings, lesions to the right hemisphere following stroke have long been known to cause more severe and long-lasting deficits in eye movements compared with left hemisphere lesions (De Renzi et al. 1982; Perry and Zeki 2000). Indeed, hemispheric lateralization has been found for many cognitive functions, most notably within the language domain (Powell et al. 2006; Catani et al. 2007; Vernooij et al. 2007) and appears to be a uniquely defining feature of the human brain—thought to accompany the evolutionary advance in cognitive ability (Hopkins and Rilling 2000; Vallortigara and Rogers 2005). In contrast, anatomical and functional aspects of the macaque brain are largely symmetrical, and lesions to the right or left hemisphere cause comparable deficits (Gaffan and Hornak 1997; Kagan et al. 2010).

Similar right hemisphere dominance also exists within the network for spatial attention in the human brain (Kim et al. 1999; Mesulam 1999; Bartolomeo et al. 2007; Umarova et al. 2010) and given the intimate relationship that exists between spatial attention and eye movements (Corbetta et al. 1998; Nobre et al. 2000), perhaps it is not surprising that we find similar lateralization for the oculomotor system. Anatomical connections underlying the oculomotor system may well be shared with those for orienting attention when an oculomotor response is required (Umarova et al. 2010).

Structural connectivity studies in monkeys have highlighted the importance of the long association fibers of the superior longitudinal fasciculus (SLF) in spatial processing (Mesulam 1981; Petrides and Pandya 2006; Schmahmann et al. 2007), these fibers connect the frontal lobe to the parietal, temporal and occipital lobes, and similar frontoparietal pathways have been identified within the human brain (Catani et al. 2002; Makris et al. 2005; Thiebaut de Schotten et al. 2005; Doricchi

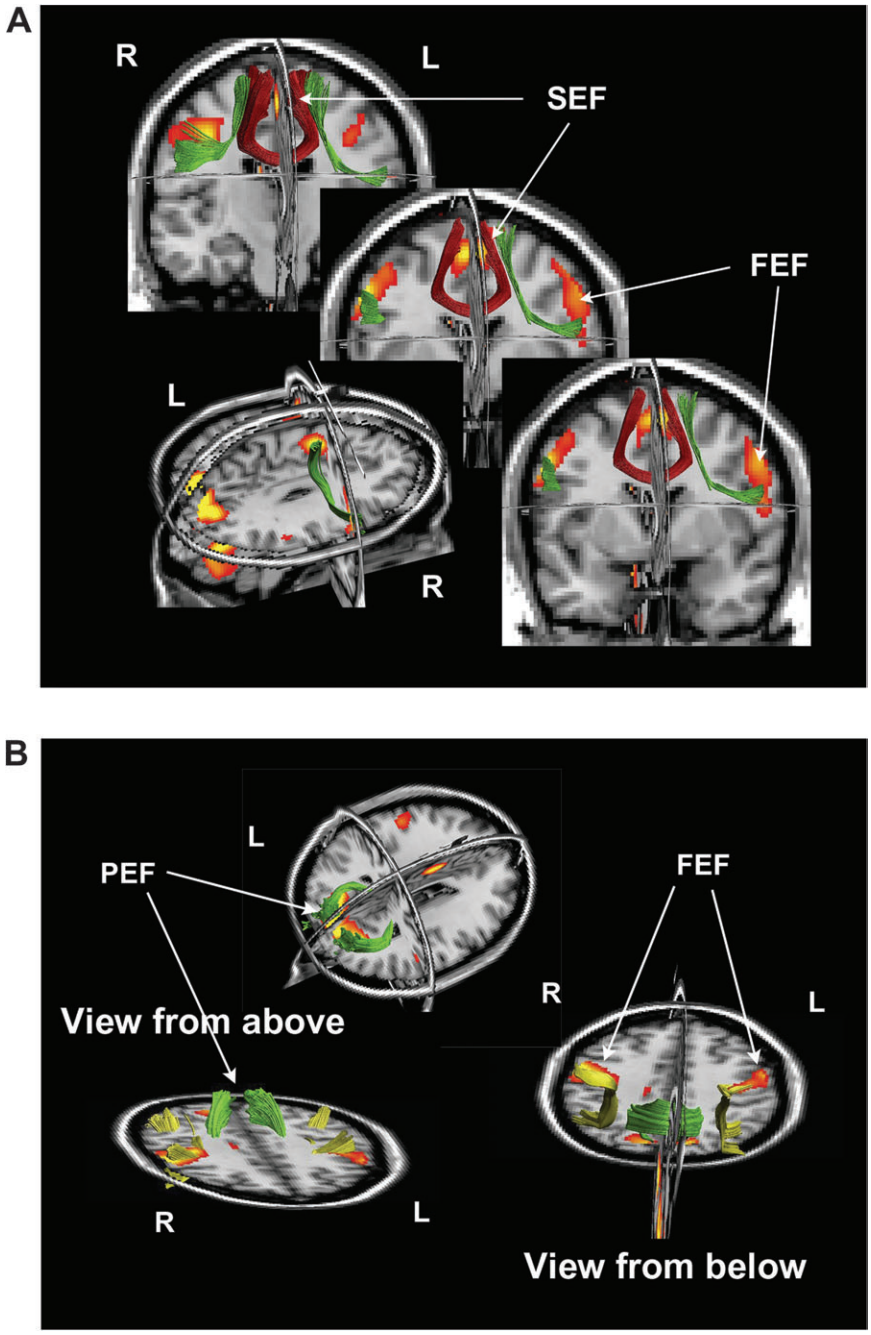

Figure 5. Reconstructed tracts for the group average data set. Reconstructed tracts are illustrated in 3D superimposed on coronal, axial, and sagittal slices of the SPM T_1 template image, together with the group fMRI results (RFX analysis, illustrated at $P = 0.005$), all normalized and coregistered in MNI space. (*A*) Reconstructed pathways within the frontal lobes—tract connecting contralateral SEF shown in red, ipsilateral SEF to FEF connections shown in green. (*B*) Parietal connections—contralateral PEF connections are illustrated in green and the lateral tract connecting ipsilateral FEF and inferior parietal cortex is shown in yellow. Unlike all the other tracts described, this latter tract does not terminate in a region of cortex activated by our oculomotor task. Instead this lateral tract terminates in the inferior parietal cortex, near the junction of the angular gyrus and supramarginal gyrus (homologous to BAs 39/40): approximate MNI coordinates: L [−38/−62/46], R [41/−55/46]—an area known to be involved in visually guided saccades. This figure was generated using "ExploreDTI" (Leemans et al. 2009).

et al. 2008; Gharabaghi et al. 2009; Bernal and Altman 2010). The right lateralized frontoparietal pathway dissected here, has closest homology with the middle segment of the SLF-II, which connects the dorsolateral prefrontal cortex to the inferior parietal cortex. Damage to this pathway within the right hemisphere results in visual neglect and a profound deficit in orienting and sustaining spatial attention toward contralateral space (Mort, Malhotra, et al. 2003; Bartolomeo et al. 2007; Husain and Nachev 2007; Shinoura et al. 2009; Singh-Curry and Husain 2009). The right inferior parietal region to which the FEF connects is known to be involved in visually guided oculomotor tasks (Perry and Zeki 2000; Mort, Perry, et al. 2003; Petit et al. 2009; Kagan et al. 2010), when the target for an eye movement is visible and needs to be spatially mapped. However, this area was not consistently activated by the oculomotor task we employed here, which required voluntary

eye movements to be performed in the dark, that is, in the absence of a visual target.

Our interpretation relies on the assumption that the output of the tractography algorithm is a true reflection of the corresponding white matter tracts, and that any reconstructed fibers projecting toward a region of cortical activity will ultimately synapse in that region and hence are direct evidence of an anatomical connection. However, we acknowledge that this is a noninvasive technique, and with the currently achievable image resolution and the complex architecture in juxtacortical white matter, it is possible that fibers that appear to project to specific regions of cortex may not actually terminate there. Nevertheless, we believe tractography provides us with the best possible insights into white matter tracts in the living human brain that cannot currently be achieved by any other modality.

Although we have successfully dissected white matter pathways connecting key oculomotor regions in the human brain, it is of course possible that additional connections exist that have not been identified here. For example, a direct pathway between the FEF and the superior parietal cortex might have been expected, based on anatomical findings in macaque (Huerta et al. 1987; Stanton et al. 1995), as well as fMRI studies in humans that demonstrate simultaneous activity in these regions during eye movements and spatial orienting tasks (Corbetta 1998; Natale et al. 2009). It is possible that alternative tractography approaches such as spherical deconvolution based techniques (Frank 2001; Tournier et al. 2004; Dell'acqua et al. 2010; Jeurissen et al. 2011), may yield different results—especially in areas of complex fiber architecture. However, such methods have their own limitations and shortcomings (for review, see Tournier et al. 2011). For instance, bending single fiber bundle populations (i.e., pathways with high curvature at the length scale of the voxel size) could be perceived as multiple fiber populations by these alternative approaches. As this is an active field of research, it currently remains unclear how this will affect the identification of specific pathways within complex fiber systems.

By combining information from both fMRI and diffusion MRI–based tractography, we have found strong support for the existence of key structural links between cortical areas involved in gaze control in humans. This critical information not only allows us to explore similarities and differences between species, it provides a basis for constraining future exploration into the functional role of these connections, and whether such connectivity modulates with task requirements. Furthermore, within a clinical setting, combined tractography and fMRI can be used to assess changes in network configuration that might occur following brain damage or as a result of subsequent neurological treatment (Grefkes et al. 2010). Such information could be used to constrain as well as monitor the progress of different methods of treatment and rehabilitation.

Previous multimodel imaging studies have defined regions of cortex identified using fMRI to constrain tractography algorithms. However, only one of these studies used an initial unconstrained anatomically guided approach, followed by fMRI-constrained path reconstruction (Conturo et al. 1999). In addition, with one exception (Powell et al. 2006), these studies did not seek to establish the existence of hemispheric bias, and hence did not control for hemispheric difference in the size of the seed ROIs or else chose to examine just one hemisphere (Upadhyay et al. 2007; Umarova et al. 2010). Here, we performed both anatomically guided and fMRI-constrained path reconstructions, using controlled methods to ensure no loss of information due to variability in individual anatomy as well as preventing the possibility that hemisphere bias in seed definition could have been introduced by the operator.

Conclusions

We combined diffusion MRI–based tractography with fMRI to explore white matter connections within the human oculomotor system. Our data provide compelling support for the existence of white matter pathways that have previously only been described in detail in nonhuman primates. In addition, we highlight an important new finding that appears to be unique to humans—that is, a significant right hemisphere bias in the white matter pathways connecting oculomotor control centers. This lateralization exists for connections within the frontal lobes, as well as between the frontal and parietal lobes.

Funding

The Wellcome Trust (grant number 061140).

Notes

Conflict of Interest: None declared.

References

Alexander DC, Gee JC, Bajesy R. 1999. Strategies for data reorientation during non-rigid transformations of diffusion tensor images. In: Taylor CJ and Colchester ACF, editors. Proceedings of the second International Conference on Medical Image Computing and Computer-Assisted Intervention, Cambridge, UK; 1999 Sep 19–22; Springer.

Amiez C, Petrides M. 2009. Anatomical organization of the eye fields in the human and non-human primate frontal cortex. Prog Neurobiol. 89:220–230.

Anderson EJ, Husain M, Sumner P. 2008. Human intraparietal sulcus (IPS) and competition between exogenous and endogenous saccade plans. Neuroimage. 40:838–851.

Bartolomeo P, Thiebaut de Schotten M, Doricchi F. 2007. Left unilateral neglect as a disconnection syndrome. Cereb Cortex. 17:2479–2490.

Basser PJ, Mattiello J, LeBihan D. 1994. MR diffusion tensor spectroscopy and imaging. Biophys J. 66:259–267.

Basser PJ, Pajevic S, Pierpaoli C, Duda J, Aldroubi A. 2000. In vivo fiber tractography using DT-MRI data. Magn Reson Med. 44:625–632.

Basser PJ, Pierpaoli C. 1996. Microstructural and physiological features of tissues elucidated by quantitative-diffusion-tensor MRI. J Magn Reson B. 111:209–219.

Beaulieu C. 2002. The basis of anisotropic water diffusion in the nervous system—a technical review. NMR Biomed. 15:435–455.

Bernal B, Altman N. 2010. The connectivity of the superior longitudinal fasciculus: a tractography DTI study. Magn Reson Imaging. 28:217–225.

Binello A, Mannan S, Ruddock KH. 1995. The characteristics of eye movements made during visual search with multi-element stimuli. Spat Vis. 9:343–362.

Blatt GJ, Andersen RA, Stoner GR. 1990. Visual receptive field organization and cortico-cortical connections of the lateral intraparietal area (area LIP) in the macaque. J Comp Neurol. 299:421–445.

Brignani D, Bortoletto M, Miniussi C, Maioli C. 2010. The when and where of spatial storage in memory-guided saccades. Neuroimage. 52(4):1611–1620.

Broerse A, Crawford TJ, den Boer JA. 2001. Parsing cognition in schizophrenia using saccadic eye movements: a selective overview. Neuropsychologia. 39:742–756.

Bruce CJ, Goldberg ME, Bushnell MC, Stanton GB. 1985. Primate frontal eye fields. II. Physiological and anatomical correlates of electrically evoked eye movements. J Neurophysiol. 54:714–734.
Catani M, Allin MP, Husain M, Pugliese L, Mesulam MM, Murray RM, Jones DK. 2007. Symmetries in human brain language pathways correlate with verbal recall. Proc Natl Acad Sci U S A. 104:17163–17168.
Catani M, ffytche DH. 2005. The rises and falls of disconnection syndromes. Brain. 128:2224–2239.
Catani M, Howard RJ, Pajevic S, Jones DK. 2002. Virtual in vivo interactive dissection of white matter fasciculi in the human brain. Neuroimage. 17:77–94.
Conturo TE, Lori NF, Cull TS, Akbudak E, Snyder AZ, Shimony JS, McKinstry RC, Burton H, Raichle ME. 1999. Tracking neuronal fiber pathways in the living human brain. Proc Natl Acad Sci U S A. 96:10422–10427.
Corbetta M. 1998. Frontoparietal cortical networks for directing attention and the eye to visual locations: identical, independent, or overlapping neural systems? Proc Natl Acad Sci U S A. 95:831–838.
Corbetta M, Akbudak E, Conturo TE, Snyder AZ, Ollinger JM, Drury HA, Linenweber MR, Petersen SE, Raichle ME, Van Essen DC, et al. 1998. A common network of functional areas for attention and eye movements. Neuron. 21:761–773.
De Renzi E, Colombo A, Faglioni P, Gibertoni M. 1982. Conjugate gaze paresis in stroke patients with unilateral damage. An unexpected instance of hemispheric asymmetry. Arch Neurol. 39:482–486.
Dell'acqua F, Scifo P, Rizzo G, Catani M, Simmons A, Scotti G, Fazio F. 2010. A modified damped Richardson-Lucy algorithm to reduce isotropic background effects in spherical deconvolution. Neuroimage. 49:1446–1458.
Doricchi F, Thiebaut de Schotten M, Tomaiuolo F, Bartolomeo P. 2008. White matter (dis)connections and gray matter (dys)functions in visual neglect: gaining insights into the brain networks of spatial awareness. Cortex. 44:983–995.
Frank LR. 2001. Anisotropy in high angular resolution diffusion-weighted MRI. Magn Reson Med. 45:935–939.
Friston KJ, Holmes AP, Worsley KJ. 1999. How many subjects constitute a study? Neuroimage. 10:1–5.
Gaffan D, Hornak J. 1997. Visual neglect in the monkey. Representation and disconnection. Brain. 120(Pt 9):1647–1657.
Gharabaghi A, Kunath F, Erb M, Saur R, Heckl S, Tatagiba M, Grodd W, Karnath HO. 2009. Perisylvian white matter connectivity in the human right hemisphere. BMC Neurosci. 10:15.
Goldberg ME, Bisley J, Powell KD, Gottlieb J, Kusunoki M. 2002. The role of the lateral intraparietal area of the monkey in the generation of saccades and visuospatial attention. Ann N Y Acad Sci. 956:205–215.
Goldman-Rakic PS. 1988. Topography of cognition: parallel distributed networks in primate association cortex. Annu Rev Neurosci. 11:137–156.
Gooding DC, Basso MA. 2008. The tell-tale tasks: a review of saccadic research in psychiatric patient populations. Brain Cogn. 68:371–390.
Grefkes C, Wang LE, Eickhoff SB, Fink GR. 2010. Noradrenergic modulation of cortical networks engaged in visuomotor processing. Cereb Cortex. 20:783–797.
Grosbras MH, Lobel E, Van de Moortele PF, LeBihan D, Berthoz A. 1999. An anatomical landmark for the supplementary eye fields in human revealed with functional magnetic resonance imaging. Cereb Cortex. 9:705–711.
Hagmann P, Cammoun L, Gigandet X, Meuli R, Honey CJ, Wedeen VJ, Sporns O. 2008. Mapping the structural core of human cerebral cortex. PLoS Biol. 6:e159.
Hopkins WD, Rilling JK. 2000. A comparative MRI study of the relationship between neuroanatomical asymmetry and interhemispheric connectivity in primates: implication for the evolution of functional asymmetries. Behav Neurosci. 114:739–748.
Huerta MF, Krubitzer LA, Kaas JH. 1987. Frontal eye field as defined by intracortical microstimulation in squirrel monkeys, owl monkeys, and macaque monkeys. II. Cortical connections. J Comp Neurol. 265:332–361.
Husain M, Mannan S, Hodgson T, Wojciulik E, Driver J, Kennard C. 2001. Impaired spatial working memory across saccades contributes to abnormal search in parietal neglect. Brain. 124:941–952.
Husain M, Nachev P. 2007. Space and the parietal cortex. Trends Cogn Sci. 11:30–36.
Jeurissen B, Leemans A, Jones DK, Tournier JD, Sijbers J. 2011. Probabilistic fiber tracking using the residual bootstrap with constrained spherical deconvolution. Hum Brain Mapp. 32:461–479.
Johnston K, Everling S. 2008. Neurophysiology and neuroanatomy of reflexive and voluntary saccades in non-human primates. Brain Cogn. 68:271–283.
Jones DK. 2008. Studying connections in the living human brain with diffusion MRI. Cortex. 44:936–952.
Jones DK, Griffin LD, Alexander DC, Catani M, Horsfield MA, Howard R, Williams SC. 2002. Spatial normalization and averaging of diffusion tensor MRI data sets. Neuroimage. 17:592–617.
Jones DK, Simmons A, Williams SC, Horsfield MA. 1999. Non-invasive assessment of axonal fiber connectivity in the human brain via diffusion tensor MRI. Magn Reson Med. 42:37–41.
Jones DK, Williams SC, Gasston D, Horsfield MA, Simmons A, Howard R. 2002. Isotropic resolution diffusion tensor imaging with whole brain acquisition in a clinically acceptable time. Hum Brain Mapp. 15:216–230.
Kagan I, Iyer A, Lindner A, Andersen RA. 2010. Space representation for eye movements is more contralateral in monkeys than in humans. Proc Natl Acad Sci U S A. 107:7933–7938.
Kennard C, Mannan SK, Nachev P, Parton A, Mort DJ, Rees G, Hodgson TL, Husain M. 2005. Cognitive processes in saccade generation. Ann N Y Acad Sci. 1039:176–183.
Kim DS, Kim M. 2005. Combining functional and diffusion tensor MRI. Ann N Y Acad Sci. 1064:1–15.
Kim YH, Gitelman DR, Nobre AC, Parrish TB, LaBar KS, Mesulam MM. 1999. The large-scale neural network for spatial attention displays multifunctional overlap but differential asymmetry. Neuroimage. 9:269–277.
Lanyon LJ, Giaschi D, Young SA, Fitzpatrick K, Diao L, Bjornson BH, Barton JJ. 2009. Combined functional MRI and diffusion tensor imaging analysis of visual motion pathways. J Neuroophthalmol. 29:96–103.
Leemans A, Jeurissen B, Sijbers J, Jones DK. 2009. ExploreDTI: a graphical toolbox for processing, analyzing, and visualizing diffusion MR data. International Society for Magnetic Resonance in Medicine—17th Scientific Meeting; 2009 Apr 18–24; Honolulu, Hawaii, USA .
Leemans A, Jones DK. 2009. The B-matrix must be rotated when correcting for subject motion in DTI data. Magn Reson Med. 61:1336–1349.
Levy I, Schluppeck D, Heeger DJ, Glimcher PW. 2007. Specificity of human cortical areas for reaches and saccades. J Neurosci. 27:4687–4696.
Lobel E, Kahane P, Leonards U, Grosbras M, Lehericy S, Le Bihan D, Berthoz A. 2001. Localization of human frontal eye fields: anatomical and functional findings of functional magnetic resonance imaging and intracerebral electrical stimulation. J Neurosurg. 95:804–815.
Makris N, Kennedy DN, McInerney S, Sorensen AG, Wang R, Caviness VS, Jr., Pandya DN. 2005. Segmentation of subcomponents within the superior longitudinal fascicle in humans: a quantitative, in vivo, DT-MRI study. Cereb Cortex. 15:854–869.
Mannan SK, Mort DJ, Hodgson TL, Driver J, Kennard C, Husain M. 2005. Revisiting previously searched locations in visual neglect: role of right parietal and frontal lesions in misjudging old locations as new. J Cogn Neurosci. 17:340–354.
McDowell JE, Dyckman KA, Austin BP, Clementz BA. 2008. Neurophysiology and neuroanatomy of reflexive and volitional saccades: evidence from studies of humans. Brain Cogn. 68:255–270.
Mesulam MM. 1981. A cortical network for directed attention and unilateral neglect. Ann Neurol. 10:309–325.
Mesulam MM. 1999. Spatial attention and neglect: parietal, frontal and cingulate contributions to the mental representation and attentional targeting of salient extrapersonal events. Philos Trans R Soc Lond B Biol Sci. 354:1325–1346.

Mori S, Crain BJ, Chacko VP, van Zijl PC. 1999. Three-dimensional tracking of axonal projections in the brain by magnetic resonance imaging. Ann Neurol. 45:265–269.
Mort DJ, Malhotra P, Mannan SK, Rorden C, Pambakian A, Kennard C, Husain M. 2003. The anatomy of visual neglect. Brain. 126: 1986–1997.
Mort DJ, Perry RJ, Mannan SK, Hodgson TL, Anderson E, Quest R, McRobbie D, McBride A, Husain M, Kennard C. 2003. Differential cortical activation during voluntary and reflexive saccades in man. Neuroimage. 18:231–246.
Natale E, Marzi CA, Macaluso E. 2009. FMRI correlates of visuo-spatial reorienting investigated with an attention shifting double-cue paradigm. Hum Brain Mapp. 30:2367–2381.
Nobre AC, Gitelman DR, Dias EC, Mesulam MM. 2000. Covert visual spatial orienting and saccades: overlapping neural systems. Neuroimage. 11:210–216.
Paus T. 1996. Location and function of the human frontal eye-field: a selective review. Neuropsychologia. 34:475–483.
Perry RJ, Zeki S. 2000. The neurology of saccades and covert shifts in spatial attention: an event-related fMRI study. Brain. 123(Pt 11):2273–2288.
Petit L, Zago L, Vigneau M, Andersson F, Crivello F, Mazoyer B, Mellet E, Tzourio-Mazoyer N. 2009. Functional asymmetries revealed in visually guided saccades: an FMRI study. J Neurophysiol. 102:2994–3003.
Petrides M, Pandya DN. 2006. Efferent association pathways originating in the caudal prefrontal cortex in the macaque monkey. J Comp Neurol. 498:227–251.
Posner MI, Walker JA, Friedrich FJ, Rafal RD. 1984. Effects of parietal injury on covert orienting of attention. J Neurosci. 4:1863–1874.
Powell HW, Parker GJ, Alexander DC, Symms MR, Boulby PA, Wheeler-Kingshott CA, Barker GJ, Noppeney U, Koepp MJ, Duncan JS. 2006. Hemispheric asymmetries in language-related pathways: a combined functional MRI and tractography study. Neuroimage. 32: 388–399.
Rafal RD. 1994. Neglect. Curr Opin Neurobiol. 4:231–236.
Russo GS, Bruce CJ. 2000. Supplementary eye field: representation of saccades and relationship between neural response fields and elicited eye movements. J Neurophysiol. 84:2605–2621.
Rykhlevskaia E, Gratton G, Fabiani M. 2008. Combining structural and functional neuroimaging data for studying brain connectivity: a review. Psychophysiology. 45:173–187.
Saur D, Kreher BW, Schnell S, Kummerer D, Kellmeyer P, Vry MS, Umarova R, Musso M, Glauche V, Abel S, et al. 2008. Ventral and dorsal pathways for language. Proc Natl Acad Sci U S A. 105:18035–18040.
Schall JD, Morel A, King DJ, Bullier J. 1995. Topography of visual cortex connections with frontal eye field in macaque: convergence and segregation of processing streams. J Neurosci. 15:4464–4487.
Schluppeck D, Curtis CE, Glimcher PW, Heeger DJ. 2006. Sustained activity in topographic areas of human posterior parietal cortex during memory-guided saccades. J Neurosci. 26:5098–5108.
Schluppeck D, Glimcher P, Heeger DJ. 2005. Topographic organization for delayed saccades in human posterior parietal cortex. J Neurophysiol. 94:1372–1384.
Schmahmann JD, Pandya DN. 2006. Fiber pathways of the brain. Oxford: Oxford University Press.
Schmahmann JD, Pandya DN, Wang R, Dai G, D'Arceuil HE, de Crespigny AJ, Wedeen VJ. 2007. Association fibre pathways of the brain: parallel observations from diffusion spectrum imaging and autoradiography. Brain. 130:630–653.
Sereno MI, Pitzalis S, Martinez A. 2001. Mapping of contralateral space in retinotopic coordinates by a parietal cortical area in humans. Science. 294:1350–1354.
Shinoura N, Suzuki Y, Yamada R, Tabei Y, Saito K, Yagi K. 2009. Damage to the right superior longitudinal fasciculus in the inferior parietal lobe plays a role in spatial neglect. Neuropsychologia. 47:2600–2603.
Singh-Curry V, Husain M. 2009. The functional role of the inferior parietal lobe in the dorsal and ventral stream dichotomy. Neuropsychologia. 47:1434–1448.
Sporns O, Tononi G, Kotter R. 2005. The human connectome: a structural description of the human brain. PLoS Comput Biol. 1e42.
Staempfli P, Reischauer C, Jaermann T, Valavanis A, Kollias S, Boesiger P. 2008. Combining fMRI and DTI: a framework for exploring the limits of fMRI-guided DTI fiber tracking and for verifying DTI-based fiber tractography results. Neuroimage. 39:119–126.
Stanton GB, Bruce CJ, Goldberg ME. 1993. Topography of projections to the frontal lobe from the macaque frontal eye fields. J Comp Neurol. 330:286–301.
Stanton GB, Bruce CJ, Goldberg ME. 1995. Topography of projections to posterior cortical areas from the macaque frontal eye fields. J Comp Neurol. 353:291–305.
Sumner P, Nachev P, Castor-Perry S, Isenman H, Kennard C. 2006. Which visual pathways cause fixation-related inhibition? J Neurophysiol. 95:1527–1536.
Sweeney JA, Luna B, Keedy SK, McDowell JE, Clementz BA. 2007. fMRI studies of eye movement control: investigating the interaction of cognitive and sensorimotor brain systems. Neuroimage. 36(Suppl 2):T54–T60.
Tehovnik EJ, Sommer MA, Chou IH, Slocum WM, Schiller PH. 2000. Eye fields in the frontal lobes of primates. Brain Res Brain Res Rev. 32:413–448.
Thiebaut de Schotten M, Urbanski M, Duffau H, Volle E, Levy R, Dubois B, Bartolomeo P. 2005. Direct evidence for a parietal-frontal pathway subserving spatial awareness in humans. Science. 309:2226–2228.
Thier P, Andersen RA. 1998. Electrical microstimulation distinguishes distinct saccade-related areas in the posterior parietal cortex. J Neurophysiol. 80:1713–1735.
Tournier JD, Calamante F, Gadian DG, Connelly A. 2004. Direct estimation of the fiber orientation density function from diffusion-weighted MRI data using spherical deconvolution. Neuroimage. 23:1176–1185.
Tournier JD, Mori S, Leemans A. Diffusion Tensor Imaging and Beyond. Magnetic Resonance in Medicine. 65:1532–1556.
Umarova RM, Saur D, Schnell S, Kaller CP, Vry MS, Glauche V, Rijntjes M, Hennig J, Kiselev V, Weiller C. 2010. Structural connectivity for visuospatial attention: significance of ventral pathways. Cereb Cortex. 20:121–129.
Upadhyay J, Ducros M, Knaus TA, Lindgren KA, Silver A, Tager-Flusberg H, Kim DS. 2007. Function and connectivity in human primary auditory cortex: a combined fMRI and DTI study at 3 Tesla. Cereb Cortex. 17:2420–2432.
Vallortigara G, Rogers LJ. 2005. Survival with an asymmetrical brain: advantages and disadvantages of cerebral lateralization. Behav Brain Sci. 28:575–589discussion 589–633.
Vernooij MW, Smits M, Wielopolski PA, Houston GC, Krestin GP, van der Lugt A. 2007. Fiber density asymmetry of the arcuate fasciculus in relation to functional hemispheric language lateralization in both right- and left-handed healthy subjects: a combined fMRI and DTI study. Neuroimage. 35:1064–1076.
Woods RP, Grafton ST, Holmes CJ, Cherry SR, Mazziotta JC. 1998. Automated image registration: I. General methods and intrasubject, intramodality validation. J Comput Assist Tomogr. 22:139–152.
Woods RP, Grafton ST, Watson JD, Sicotte NL, Mazziotta JC. 1998. Automated image registration: II. Intersubject validation of linear and nonlinear models. J Comput Assist Tomogr. 22:153–165.
Zhang S, Demiralp C, Laidlaw D. 2003. Visualising diffusion tensor MR images using streamtubes and streamsurfaces. IEEE Trans Vis Comput Graph. 9(4):454–462.